International Journal of Fluid Power 6 (2005) No. 2 pp. 5-18

INFLUENCE OF NOTCH SHAPE AND NUMBER OF NOTCHES ON THE METERING CHARACTERISTICS OF HYDRAULIC SPOOL VALVES

[1] Massimo Borghi, [1] Massimo Milani, [2] Roberto Paoluzzi

[1] Department of Mechanical and Civil Engineering – University of Modena & Reggio Emilia
Via Vignolese, 905/b – 41100 Modena – Italy
[2] IMAMOTER – CNR
Via Canal Bianco 28 - 44044 Cassana (Ferrara) - Italy

Abstract

The paper presents theoretical and experimental results of studies on the influence of shape and number of spool notches on the discharge characteristics (discharge coefficient, velocity coefficient and flow angle) of a hydraulic distributor metering edge.

The flow-rate vs. pressure drop and the steady state axial flow-force vs. pressure drop diagrams are determined for spools with different configurations of multiple notched metering edges. Various combinations of the shape and number of the notches modulating the metering area of the passage between supply and drain ports were investigated and correlated with flow-rate, axial flow-force and pressure drop, in order to get estimates of discharge coefficient and flow angle.

The procedure is applied to all the data collected during the experimental activity, and shows the behaviour of the flow characteristics in both the fully turbulent and transitional region of motion. The influence of notch shape and number on the metering edge flow characteristics is evaluated as well.

Keywords: Hydraulic components, spool valves, metering edge, metering notches, experimental characterization, discharge coefficient, axial flow-forces

1 Introduction

The modulation of fluid power, in modern electro-hydraulic systems for both industrial and mobile application, is obtained by proper metering characteristics of the notches in the metering edge of the valve spool.

The design of this type of components and the simulation of their steady state and dynamic behaviour, is made difficult by the peculiarities of flow conditions as a function of metering area and by the complex dependencies on fluid flow. In the early 60s' pioneering studies carried out at M.I.T. focused the attention of researchers on the fundamental role played by the variability of discharge coefficient and efflux angle on the behaviour of a metering edge. This was found to affect significantly the variation of power modulation function performed. The effect of metering edge geometry and of spool-seat coupling were highlighted by Blackburn et al. (1960) and in Merritt (1967). Viersma (1980) describes the role played by stationary and dynamic efflux characteristics in hydraulic servo-systems, where the transition from laminar to fully turbulent flow is handled by a tailored function describing the variation of the discharge coefficient. The experimental study presented by Johnston et al. (1991) details on one hand the effect of the shape on the metering characteristics of poppet and disk valves, on the other highlights, in particular for fully turbulent flows, how the design parameters could influence these characteristics, mainly in terms of flow forces acting on the moving element. The detailed experimental investigation carried out by Lugowsky (1993), shows that axial flow forces, and consequently discharge characteristics, are conditioned not only by opening of the metering edge, but also by geometries of spool and seat and by other factors, like the Coanda effect.

The ever increasing demand for numerical tools for sizing and simulation of fluid power components, forced many researchers to address the topic of characterization of static and dynamic flows of incompressible fluid through geometries representing the metering edge of hydraulic valves. Several papers by the Authors were devoted to Computational Fluid Dynamics (CFD) simulation and to experimental verification of typical

This manuscript was received on 21 September 2004 and was accepted after revision for publication on 17 June 2005

discharge coefficient values found in industrial components. They reported results on sharp edged geometries (Borghi et al., 1996, 1997 and 1998), conic profile (Borghi et al., 1999) and on typical 'compensated' profile for the minimization of axial flow forces (Borghi et al., 2000). Work by Ellmann and Piche (1996) and Wu et al. (2002), was concerned with developing a semi-empirical expression describing the variability of the discharge coefficients in fixed-geometry orifices. Wu et al. (2003) extended this work by considering the fluid flow at very small openings. All these approaches can be powerful tools for the modelling of this kind of simple components but, unfortunately, on one hand they are not directly applicable to complex shapes and, on the other hand, they need the knowledge of the saturated flow characteristics in order to give information in the whole operational envelope of the variable metering orifice. Other interesting results providing a better insight into the problem have been obtained by Elgamil (2001), Gromala et al. (2002) and Del Vescovo and Lippolis (2002).

The results presented in this paper are concerned with steady-state analysis of metering edges with notches. The aim of the paper is to show what effect the shape and number of notches may have on the discharge characteristics of orifices under different operating conditions.

The first part of the paper presents the experimental set-up used. Eight different spools with different notches have been tested over a wide range of input hydraulic power. The shape of the grooves was derived from typical industrial designs and metering edges had two, three or four grooves. Experimental data have been used to estimate the characteristic of a given metering edge and, consequently, the discharge coefficient and efflux angle variations as a function of flow conditions. The investigation drives to the definition of both saturation values for discharge characteristics and variation of coefficients as a function of shape and number of considered notches.

2 Experimental Analysis

The hydraulic components for industrial application show a wide variety of notch types. The notches are designed to control hydraulic power supplied to actuators, by varying the area of the metering edge. The shape of these notches, as well as their number and angular position, affect the dynamic behaviour of the fluid, as they determine the input/output jet angles and discharge coefficient. The angular position of the notches determines the symmetry of the flow through the orifice.

Among the large number of possible edge configurations, only the three notch shapes shown in Fig. 1 have been considered for the experimental investigation. The first notch, Fig. 1-TYPE A, has a rectangular shape ended by a semicircle, the second, Fig. 1-TYPE B, is obtained by connecting three semicircles with very short rectangles (not visible in Fig. 1), while the third notch, Fig. 1-TYPE C, has a triangular section, in both axial and radial direction.

As shown in Fig. 1, the three different types of notches have the same axial length (5.25 mm), radial depth (2.20 mm), and overlap when the spool is centered (2.25 mm). All the prototypes were built with a high control on dimensional tolerances, maintaining the radial clearance between spool and sleeve less than 5 μm, and the error in metering edge opening less than 0.1 mm. This choice of clearance and positional error permits use of standard, commercial spools in test rig, and focusing of the research on the influence of the area gradient on the orifice flow characteristics.

In order to study the influence of notch number and their angular positions, three different configurations were designed and tested: two notches at 180°, three notches at 120° and four notches at 90° angular spacing.

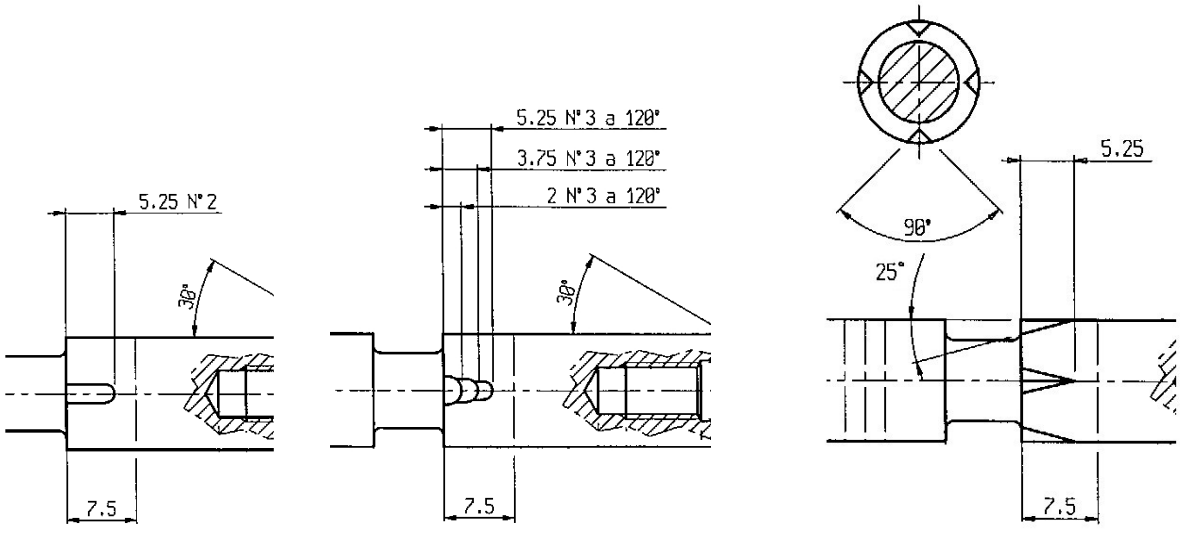

Fig. 1: *The notch shapes designed to perform the efflux characteristics experimental characterisation*

The experiments were carried out using the test bench presented in Fig. 2. The circuit schematic is shown in Fig. 2-a. A variable displacement pump (2) is connected to a volumetric flow-meter measuring the flow-rate supplied by the pump (3, range 0-150 l/min, class 0.2 absolute) to a variable orifice (6) representing the metering edge, and to a second volumetric flow-meter (10, range 0-150 l/min, class 0.2 absolute). The supply pressure is set by a relief valve (5), and the pressure drop across the variable orifice is measured using two piezo-electric pressure transducers (4 and 7, range 0-600 bar, class 0.2 absolute). A detail of the test bench is shown in Fig. 2-b. A fine pitch worm screw is used to adjust the axial position of the notched edge under test and also to measure the axial force applied to the spool which is marked (8), (range 0-150 N, class 0.1 absolute). The equipment which supports the piezo-electric micrometer (range 0-15 mm, class 0.1 absolute) is marked (9).

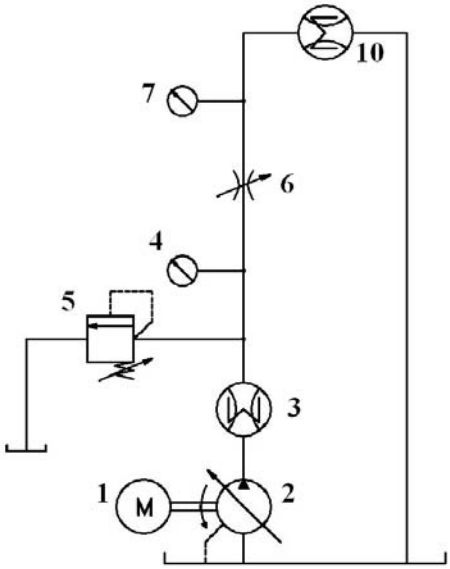

Fig. 2a: *The test bench used for the experimental activity: Circuit sketch*

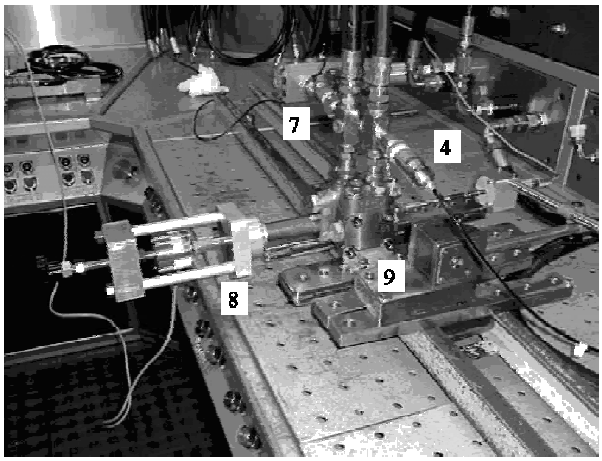

Fig. 2b: *The test bench used for the experimental activity: A detail of the mechanical equipments designed to vary and to measure the metering opening, and to measure the axial force acting on the spool*

The tests were performed in order to determine the steady-state flow-pressure characteristics of each of the eight notched edges considered. The opening of the metering edge were in the range 1 to 4 mm, in order to reduce the influence of the notch boundaries on the metering edge discharge characteristics.

Table 1 shows the openings used in the steady state characterization, for each one of the cases considered. Some of the data reported in Table 1 can be reviewed referring to Fig. 3, which shows both the axial location of some of the experimental openings along the non dimensional spool travel, and the correspondent non dimensional minimum value of the geometric area[1]. The spool displacement was non-dimensioned against maximum notch length and orifice area against its maximum value. The total efflux area was calculated, for each metering edge, as the sum of the areas geometrically defined by each notch at given spool axial travel.

As shown in Fig. 3, the steady state characteristics were collected for the metering edges designed with the Notches Type A in the following positions:

- an opening representative of the initial area gradient (in the range 1 to 1.4 mm);
- a second opening close to the area discontinuity (geometrically located 2.25 mm far from the notch opening);
- a third opening placed in the region with constant metering area.

The Notch TYPE B introduces two discontinuities into the metering area gradient, and the experimental activity was carried out in order to catch the metering edges behaviour in two extreme conditions:

- close to the discontinuity;
- in positions where discontinuity effect can be neglected.

The area function corresponding to the introduction of Notches TYPE C is quadratic with the notch opening. As shown in Fig. 3, the measurement points chosen for this edge configuration were set far from the notches boundaries, in the range between 1.60 and 3.60 mm.

The steady-state characteristic curves (namely the pressure drop vs. flow-rate curve and the axial flow-force vs. pressure drop curve) were collected for a large number of points in a range limited by the available hydraulic power (about 100 kW). The flow-rate was varied from 0 to 120 l/min and the relief valve setting from 0 to 300 bar. The steady-state characterization was performed, for each metering edge and for each metering opening, with a step by step increase in the flow-rate. Thanks to the resistance offered by the volumetric flow-meter (3), 2-4 bar of backpressure, depending on the measured flow-rate, no cavitation phenomena were detected along the discharge line, downstream the metering section.

For each operating condition, the metering edge characteristic data (the triple $Q - \Delta p - F$) was determined using the averaged values obtained during experiments. The data were collected by the acquisition

[1] This is the minimum value of the cross sectional area of the flow passage across the metering edge, evaluated at each axial spool position.

system at 250 Hz over a time interval of 0.2 s. All the data collected during the experiments are summarized in Fig. 4 to 6.

Table 1: Metering Opening Tested for the Efflux Characteristics Determination

Notch Type	Configuration	$X_{OP,A}$	$X_{OP,B}$	$X_{OP,C}$
TYPE A	2 at 180°	1.05 mm	2.30 mm	3.20 mm
	3 at 120°	1.40 mm	2.40 mm	3.40 mm
	4 at 90°	1.00 mm	2.15 mm	3.20 mm
TYPE B	2 at 180°	2.10 mm	3.00 mm	4.10 mm
	3 at 120°	1.45 mm	2.45 mm	3.45 mm
	4 at 90°	1.50 mm	2.50 mm	3.50 mm
TYPE C	2 at 180°	1.60 mm	2.60 mm	3.60 mm
	4 at 90°	1.60 mm	2.60 mm	3.60 mm

3 Saturated Efflux Characteristics of the Notched Edges

The steady-state characteristics of a metering edge as such are not a key-factor for design purposes. The main reason is that the typical operating condition of a component is dynamic, or at least non-stationary. To make the steady-state investigation effective for design purposes, it is necessary to extract information and general guidelines not directly available from the experimental evidence, such as the discharge (C_D) and the flow ($C_V \cos\theta$) coefficients variation with the metering edge geometry and the fluid flow characteristics.

Many authors (Merrit, Blackburn et al., Borghi et al., Vaughan et al., Lugowsky, Johnston et al.), show that a good design of hydraulic valves is based on:

- fluid flow coefficients characterization for all active ports;
- effect of geometry on the above mentioned coefficients;
- influence of the variation in the operating conditions on the points above.

In this perspective, the stationary characterization is a straightforward way to acquire all the information above, indirectly showing how a specific design choice might affect the flow conditions through a specific valve port. The estimated characteristic curve, in all the cases investigated, is in fairly good agreement with theoretical predictions. Flow rate vs. pressure curves are more or less quadratic with a vertex in the origin. Axial force versus pressure curve are interpolated fairly well by a line through the origin.

In this work, the experimental data have been interpolated using a third order polynomial in Q-Δp, and a first order for F-Δp.

A least square fitting procedure showed that the pressure drop can be expressed by a function of flow rate:

$$\Delta p_{EXP} = a \cdot Q_{EXP}^3 + b \cdot Q_{EXP}^2 + c \cdot Q_{EXP} \quad (1)$$

and the axial force is a function of pressure drop according to:

$$F_{EXP} = d \cdot \Delta p_{EXP} \quad (2)$$

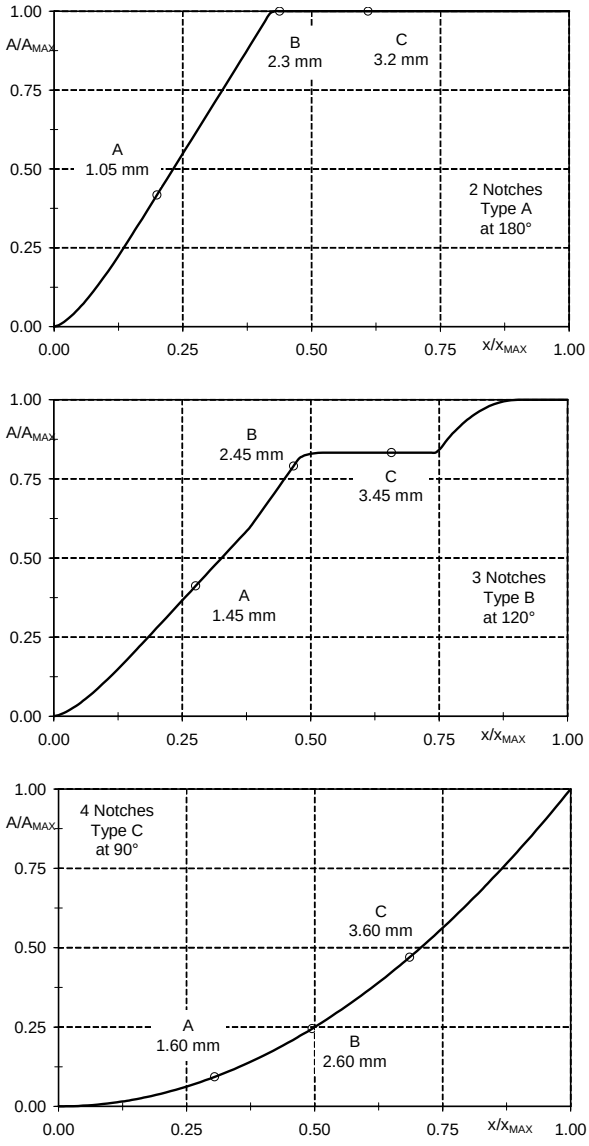

Fig. 3: *Actual Metering Opening Positions vs. Metering Edges Total Geometric Efflux Area*

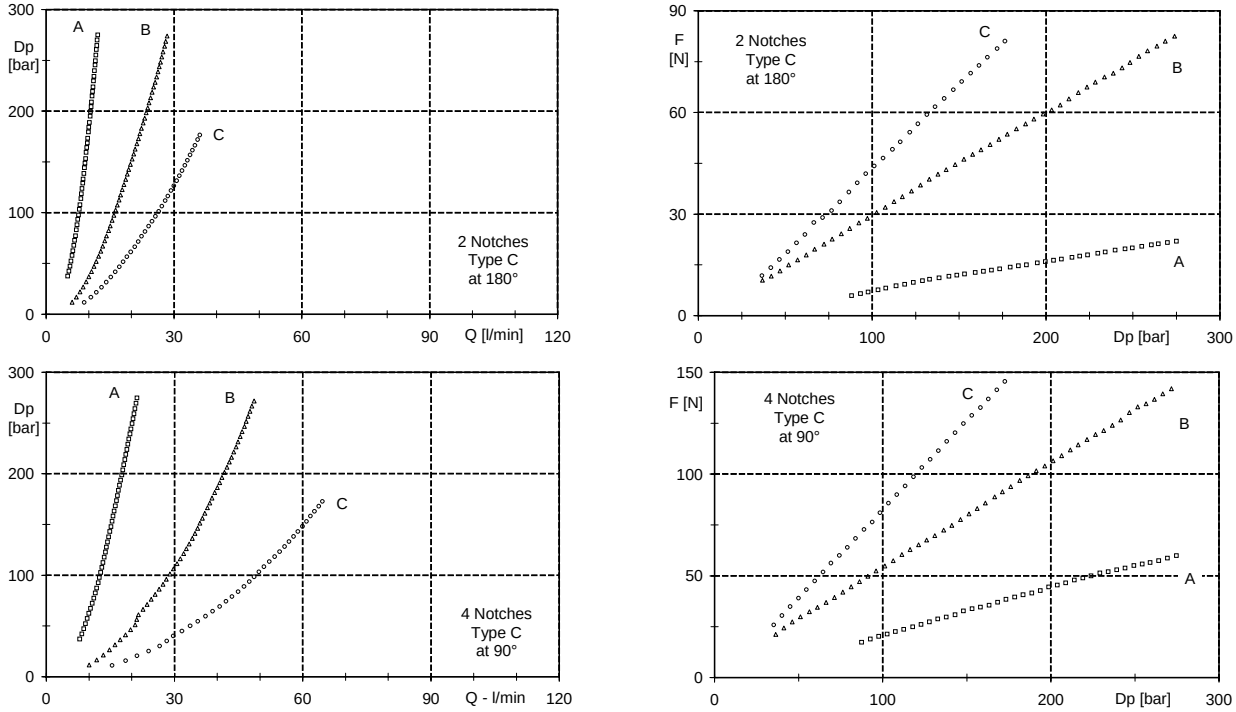

Fig. 4: *Characteristic Curves determined for the Metering Edges having 2 and 4 Notches Type C*

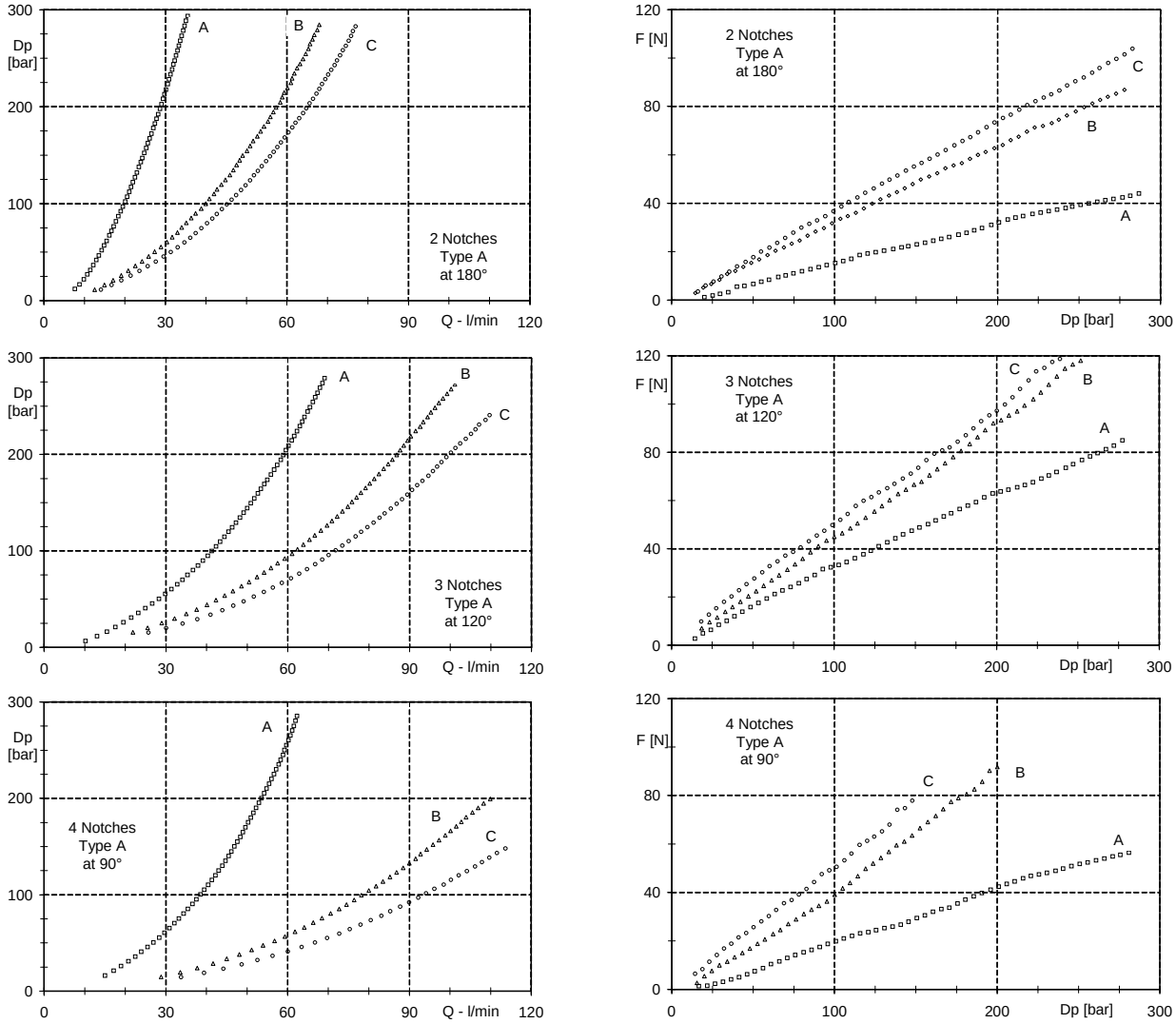

Fig. 5: *Characteristic Curves determined for the Metering Edges having 2, 3 and 4 Notches Type A*

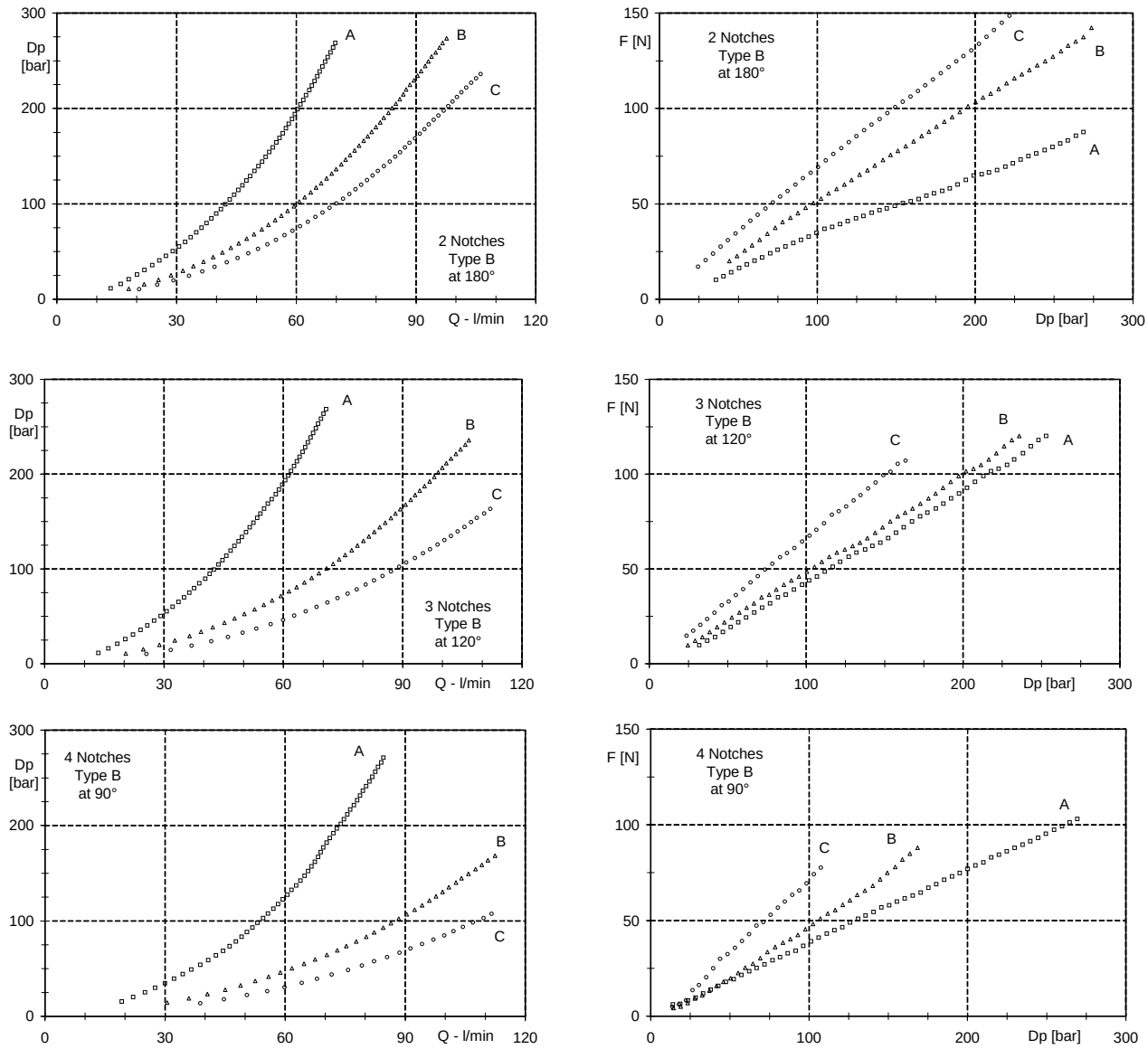

Fig. 6: *Characteristic Curves determined for the Metering Edges having 2, 3 and 4 Notches Type B*

Tables 2 to 4 show the values of the polynomial coefficients computed for all the experimental conditions examined. For the sake of simplicity, the regression coefficient *R* was not reported, but it is worth mentioning that its value is always higher than 0.9997. The fact that the *Q*-Δ*p* experimental characteristic curve is better described by third order than second order polynomials is at least partly due to measurement errors intrinsic in the instrumentation used. However, other considerations apply. The flow through a restriction can be classified, according to the amount of the flow rate, as laminar, for low Reynolds numbers, transitional and turbulent at higher Reynolds numbers. The linear relationship between *Q* and Δ*p* used for laminar flows, turns into a second order curve as the flow rate enters the turbulent range. It implies that the pressure drop could be described by the following linear combination:

$$\Delta p_{\mathrm{TH}} = a_1 \cdot Q_{\mathrm{EXP}}^2 + b_1 \cdot Q_{\mathrm{EXP}} \tag{3}$$

where linear and quadratic contributes are linearly combined to describe the overall characteristic of the restriction. In this paper, the coefficients of the linear combination are computed using a least square approximation, in order to give the best possible approximation of the curve for each notch type and opening. Tables 5 to 7 show the values of (a_1, b_1) coefficients thus determined. The regression values in this case are always higher than 0.97. Equation 3 can be rearranged as:

$$\frac{\Delta p_{\mathrm{TH}}}{Q_{\mathrm{EXP}}^2} = a_1 + \frac{b_1}{Q_{\mathrm{EXP}}} \tag{4}$$

The terms at the second member of Eq. 4 equal the square of the characteristic resistance of a turbulent orifice for an incompressible fluid, and include the correction factor fitting the actual data behaviour to the ideal parabolic correlation. The resistance is usually expressed as:

$$R_{\mathrm{T}} = \frac{1}{C_{\mathrm{D}} \cdot A_{\mathrm{GEO}} \cdot \sqrt{2/\rho}} \tag{5}$$

where C_{D} is the discharge coefficient, ρ is the fluid density (850 kg/m^3) and A_{GEO} is the reference cross sectional area of the orifice.

Table 2: Polynomial Coefficients for Experimental Data Interpolation – NOTCHES TYPE A

TYPE A	Opening	*a* [bar/(l/min)^3]	*b* [bar/(l/min)^2]	*c* [bar/(l/min)]	*d* [N/bar]
2 at 180°	A	-1.88E-03	3.13E-01	-4.75E-01	0.1557
	B	1.41E-04	4.38E-02	5.26E-01	0.3170
	C	7.71E-05	3.65E-02	3.79E-01	0.3669
3 at 120°	A	1.80E-04	3.81E-02	5.26E-01	0.3108
	B	6.04E-05	1.81E-02	2.77E-01	0.4609
	C	3.38E-05	1.52E-02	1.41E-01	0.4944
4 at 90°	A	5.19E-04	2.84E-02	7.37E-01	0.2031
	B	2.50E-05	1.30E-02	1.03E-01	0.4310
	C	1.60E-05	8.83E-03	9.97E-02	0.5121

Table 3: Polynomial Coefficients for Experimental Data Interpolation – NOTCHES TYPE B

TYPE B	Opening	*a* [bar/(l/min)^3]	*b* [bar/(l/min)^2]	*c* [bar/(l/min)]	*d* [N/bar]
2 at 180°	A	1.67E-04	3.58E-02	5.32E-01	0.3239
	B	7.45E-05	1.89E-02	2.64E-01	0.5138
	C	3.58E-05	1.59E-02	1.60E-01	0.6715
3 at 120°	A	1.01E-04	3.96E-02	4.64E-01	0.4535
	B	5.68E-05	1.21E-02	2.88E-01	0.4940
	C	2.26E-05	9.30E-03	1.34E-01	0.6622
4 at 90°	A	2.33E-04	1.17E-02	5.67E-01	0.3830
	B	3.40E-05	7.81E-03	2.01E-01	0.4849
	C	1.31E-05	6.43E-03	8.12E-02	0.6949

Table 4: Polynomial Coefficients for Experimental Data Interpolation – NOTCHES TYPE C

TYPE C	Opening	*a* [bar/(l/min)^3]	*b* [bar/(l/min)^2]	*c* [bar/(l/min)]	*d* [N/bar]
2 at 180°	A	-1.17E-02	2.41E+00	-4.79E+00	0.1167
	B	-7.01E-03	5.93E-01	-1.52E+00	0.3008
	C	-1.21E-03	1.80E-01	-5.13E-02	0.4454
4 at 90°	A	-1.44E-02	1.07E+00	-2.99E+00	0.2197
	B	-1.30E-04	1.17E-01	1.98E-01	0.5296
	C	4.29E-05	3.50E-02	2.21E-01	0.8328

Fitting the polynomials it is possible to derive the variation of the characteristic resistance as a function of the flow rate for each and every metering edge as:

$$R_T\left(Q_{EXP}\right)=\left[a_1+\frac{b_1}{Q_{EXP}}\right]^{1/2} \tag{6}$$

At the same time, the effect of the flow rate on the discharge coefficients for each metering edge is derived combining Eq. 5 and 6

$$C_D\left(Q_{EXP}\right)=\left[\frac{\rho}{2\cdot\left(a_1+b_1/Q_{EXP}\right)}\right]^{1/2}\cdot\frac{1}{A_{GEO}} \tag{7}$$

Recalling Eq. 4, it can be noted that the correction term becomes smaller and smaller as the flow rate increases, allowing the definition of a limit value for the characteristic resistance of a given geometry as:

$$R_T^{SAT}=\lim_{Q_{EXP}\to\infty}\left(\frac{\Delta p_{TH}}{Q_{EXP}^2}\right)^{1/2}=\sqrt{a_1} \tag{8}$$

This definition is obviously valid in the operating range where the flow can be considered as being fully turbulent. It can be used to compute the limit value of the discharge coefficient for a given geometry, once the flow conditions meet this turbulence criteria, i.e. Reynolds number above transitional values, corresponding to values of the discharge coefficient approximately constant. Using the definition given in Eq. 7, this limit is given by:

$$C_D^{SAT}=\lim_{Q_{EXP}\to\infty}C_D=\frac{1}{A_{GEO}}\cdot\left[\frac{\rho}{2\cdot a_1}\right]^{1/2} \tag{9}$$

The computation of the saturated discharge coefficient in all the geometries investigated, lead to the results presented in Table 8. From a general point of view, it is noted that the saturated discharge coefficient in all the cases examined is bounded between a minimum value of 0.48 and a maximum of 0.74. For notches TYPE A and B it presents a minimum value for the three notches configuration, while it decreases as the total number of notches increases for the notches TYPE C.

Notches of TYPE A show a behaviour more or less independent from their number, but strongly influenced by their axial position. Starting from values close to 0.65/0.67, for the smaller openings, C_D^{SAT} drops to 0.54/0.56 at intermediate openings and rises back to 0.62/0.64 at large openings. This is a clear effect of the discontinuity in the area function at intermediate openings, with subsequent discontinuity in the area gradient. The flow conditions are significantly affected, and the discharge coefficients decrease more than 18%. It is also worth noting that the discharge coefficient at the minimum opening of the metering edge, where the area gradient is positive, has a slightly higher value than at large openings, where the area gradient is zero.

Notches of TYPE B have a more complex area function. In this case the discharge coefficient depends on both opening and notch number. Comparing configurations having the same number of notches, the highest value of the discharge coefficient is always reached at maximum opening.

The lowest value is reached at intermediate openings in the case of three and four notches, at minimum opening for the two-notches one. Clear tendencies are not present in this case, possibly due to the complexity of the area gradient function, a piecewise linear function with two discontinuities.

As a consequence, the discharge coefficient for two notches is an increasing function of opening, from 0.62 to 0.69.

The case of three notches has a minimum value of discharge coefficient of 0.54 at intermediate openings and is 0.65 at small and large openings. The four notches configuration has a maximum value of the discharge coefficient at large openings and minimum value at intermediate openings, but shows values significantly lower (10% to 14%) than those reached in other configurations. This kind of behaviour could be the result of errors in measurements or data handling (at present not discovered by the authors), however, the absence of a systematic error only suggests that this configuration should be better investigated by means of detailed numerical simulations of the flow field which are beyond the scope of this work.

Notches of TYPE C have the highest values of the discharge coefficient at small openings. Two notches configuration always performs better than that with four notches. Discharge coefficients values decrease as the opening increases. It is worth noting that the value changes significantly during the spool travel: in the two notches configuration it drops from 0.74 to 0.57 (-23%), and in the four notches configuration from 0.70 to 0.53 (-24.3%).

Reconsidering Eq. 7, the discharge coefficient as a function of flow rate can be rearranged as:

$$\begin{aligned}C_D\left(Q_{EXP}\right)&=\frac{1}{A_{GEO}}\cdot\left[\frac{\rho}{2\cdot a_1}\right]^{1/2}\cdot\left[1+\frac{b_1}{a_1\cdot Q_{EXP}}\right]^{-1/2}\\&=C_D^{SAT}\cdot\left[1+\frac{b_1}{a_1\cdot Q_{EXP}}\right]^{-1/2}\end{aligned} \tag{10}$$

Table 5: II Order Characteristic Polynomial Coefficients – NOTCHES TYPE A

TYPE A	Opening	a_1 [bar/(l/min)^2]	b_1 [bar/(l/min)]
2 at 180°	A	0.2325	0.0064
	B	0.0612	0.0019
	C	0.0473	0.0018
3 at 120°	A	0.0520	0.01
	B	0.0265	0.0025
	C	0.0200	0.0050
4 at 90°	A	0.0718	0.0018
	B	0.0167	0.0013
	C	0.0115	0.0013

Table 6: II Order Characteristic Polynomial Coefficients – NOTCHES TYPE B

TYPE B	Opening	a_1 [bar/(l/min)^2]	b_1 [bar/(l/min)]
2 at 180°	A	0.0525	0.1417
	B	0.0289	0.0015
	C	0.0210	0.0020
3 at 120°	A	0.0510	0.2200
	B	0.0200	0.0980
	C	0.0126	0.0400
4 at 90°	A	0.0375	0.0350
	B	0.0136	0.0150
	C	0.0086	0.0030

Table 7: II Order Characteristic Polynomial Coefficients – NOTCHES TYPE C

TYPE C	Opening	a_1 [bar/(l/min)^2]	b_1 [bar/(l/min)]
2 at 180°	A	2.1000	0.3000
	B	0.3500	0.1500
	C	0.1400	0.1000
4 at 90°	A	0.5970	0.5470
	B	0.1100	0.2800
	C	0.0400	0.1340

The comparison between data on different metering edges arrangements (experimental or derived quantities) can be made using either:

- comparison of flow characteristic as a function of spool axial travel;
- comparison of flow characteristic as a function of actual cross sectional area of the equivalent orifice.

The result is that the curves must be rescaled according to a non-linear transformation which needs the definition of the area function of each and every configuration investigated. This function varies with the spool position and shows discontinuities. The only workaround to overcome these difficulties, is the introduction of a parameter able to describe the flow conditions and the geometry. The Reynolds number of a metering configuration can be defined as:

$$\mathrm{Re} = \frac{D_H \cdot (Q_{EXP}/A_{GEO})}{\nu} = \frac{4 \cdot Q_{EXP}}{\nu \cdot S} \tag{11}$$

where ν is the kinematic viscosity (32 cSt), D_H is the hydraulic diameter of the metering edge, while S is the wetted perimeter of the reference cross sectional minimum area of the orifice. It is not worthy to underline that both the hydraulic diameter and the wet perimeter vary with the metering edge opening, introducing the effect of the notched edge geometry on the Reynolds' number definition. In this way, it is possible to consider Eq. 10 in the new form:

$$C_D(\mathrm{Re}) = C_D^{SAT} \cdot \left[1 + \frac{b_1}{a_1} \cdot \frac{4}{\nu \cdot S} \cdot \frac{1}{\mathrm{Re}}\right]^{-1/2} \tag{12}$$

At the same time, the axial flow force as a function of the pressure drop across the metering edge can be expressed using the traditional Von Mises approximation (Merritt 1967 and Blackburn et al 1960):

$$F_{AX} = 2 \cdot C_D(\mathrm{Re}) \cdot A_{GEO} \cdot C_V \cdot \cos\vartheta \cdot \Delta p \tag{13}$$

Equation 13 considers as positive all forces acting towards a closure of the valve, and drives to a direct definition of the flow coefficient:

$$C_V^* = C_V \cdot \cos\vartheta \tag{14}$$

defined as the product of velocity coefficient and cosine of the jet flow angle. Combining Eq. 2 with Eq. 13 and 14, the variation of the efflux coefficient with flow conditions in the generic metering edge is given by:

$$\frac{F_{EXP}}{\Delta p_{EXP}} \cong \frac{F_{EXP}}{\Delta p_{TH}} = 2 \cdot C_D(\mathrm{Re}) \cdot A_{GEO} \cdot C_V^* = d \tag{15}$$

hence:

$$C_V^*(\mathrm{Re}) = \frac{d}{2 \cdot C_D(\mathrm{Re}) \cdot A_{GEO}} = \frac{d \cdot \left[1 + \frac{b_1}{a_1} \cdot \frac{4}{\nu \cdot S} \cdot \frac{1}{\mathrm{Re}}\right]^{1/2}}{C_D^{SAT} \cdot 2 \cdot A_{GEO}} \tag{16}$$

The flow coefficient is therefore a function of geometry and flow conditions, but it is also directly affected by the saturated value of the discharge coefficient. Equation 16 shows that the flow coefficient has a limit of $+\infty$ as Reynolds number tends to zero, indicating that the approach proposed here cannot be applied to the analysis of flow at very low Reynolds numbers. Conversely, Eq. 16 holds for the actual metering edges operating conditions, where flow can be described mainly with reference to the fully turbulent (or, at least, high transitional) conditions. In the wide range of variation of the Reynolds number where Eq. 16 holds, the flow coefficient has a saturated value defined by:

$$C_V^{*,SAT} = \lim_{\mathrm{Re}\to\infty} C_V^* = \frac{d}{C_D^{SAT} \cdot 2 \cdot A_{GEO}} \tag{17}$$

Recalling the flow coefficient definition (Eq. 14), the variation of the jet angle with the Reynolds number of the incompressible flow through a given geometry is described by the function:

$$\vartheta(\mathrm{Re}) = \arccos\left[\frac{C_V^*(\mathrm{Re})}{C_V}\right] \tag{18}$$

Which presents a saturated value expressed as:

$$\vartheta_{SAT} = \arccos\left(\frac{d}{C_V \cdot C_D^{SAT} \cdot 2 \cdot A_{GEO}}\right) \tag{19}$$

Table 9 summarizes the values of the saturated jet angle computed for all the geometries investigated.

In Eq. 19 a velocity coefficient C_V of 0.98 was used, as an average of the values found in literature.

Table 9 show that for TYPE A notches the saturated jet angle has values very close to the theoretical value found by Von Mises (69°) for an inviscid, incompressible fluid flowing from a high pressure confined volume to an unconfined volume at low pressure.

Table 8: Saturated Discharge Coefficient defined adopting the Eq. 9

TYPE A	Opening	C_D^{SAT}	TYPE B	Opening	C_D^{SAT}	TYPE C	Opening	C_D^{SAT}
2 at 180°	A	0.67	2 at 180°	A	0.62	2 at 180°	A	0.74
	B	0.55		B	0.64		B	0.69
	C	0.62		C	0.69		C	0.57
3 at 120°	A	0.67	3 at 120°	A	0.65			
	B	0.56		B	0.54			
	C	0.64		C	0.65			
4 at 90°	A	0.65	4 at 90°	A	0.55	4 at 90°	A	0.70
	B	0.54		B	0.48		B	0.61
	C	0.63		C	0.59		C	0.53

Table 9: Saturated Jet Angle defined adopting Eq. 19 (C_V = 0.98)

TYPE A	Opening	ϑ_{SAT}(°)	TYPE B	Opening	ϑ_{SAT}(°)	TYPE C	Opening	ϑ_{SAT}(°)
2 at 180°	A	69.4	2 at 180°	A	69.6	2 at 180°	A	37.4
	B	68.4		B	65.8		B	33.3
	C	68		C	62.8		C	38.5
3 at 120°	A	70.6	3 at 120°	A	61.3			
	B	69.4		B	70.8			
	C	70.8		C	69.6			
4 at 90°	A	75.2	4 at 90°	A	69.6	4 at 90°	A	37.2
	B	74.8		B	74.6		B	34.4
	C	75.0		C	72.4		C	38.6

The configuration with four notches has jet angle close to 75°, with variations as a function of spool position lower than 0.4°. Configurations with two and three notches have values, respectively close to 69° and 70°, with larger variations with spool position, but in any case lower than 1.5°.

This means that for TYPE A notches it is possible to define a unique, constant value of the saturated efflux angle, independent of the axial spool travel.

The behaviour shown by TYPE B notches is completely different. The two notches configuration shows values of ϑ_{SAT} significantly decreasing as the spool travel increases, going from 69.5° at minimum opening to 63° at maximum opening.

The three notches configuration shows the lowest ϑ_{SAT} value (approximately 61°) at minimum opening and values close to 70° at intermediate and large openings. The four notches configuration has a maximum value of ϑ_{SAT} for intermediate openings; ϑ_{SAT} values start from 69.5° at small openings, increase to 74.5° at intermediate positions and slightly decreases to 72.5° at large openings.

These results confirm that TYPE B notches have a much more complex behaviour than all the other types considered, and these anomalies can be properly understood only by a deeper investigation of the flow field inside the metering section of the valve.

TYPE C notches seem to force the saturated flow in a direction mainly determined by the radial depth of the notch, having a nominal angle of 25°, with a final nozzle effect constraining the efflux angle.

In both configurations tested (two and four notches), ϑ_{SAT} shows a similar behaviour, varying from 37.3° at small openings to 38.5° at large openings. At intermediate openings it reaches its minimum value, respectively 33.5° and 34.5°.

This configuration show no dependency on the notches number; it is therefore possible to describe all of the configuration with a single function ϑ_{SAT} of the spool position.

4 Analysing the Main Features of Notched Edges Flow Characteristics

As shown by Eq. 12 and 18, the experimental data set collect the stationary characterization of all the metering edges considered in this work. Their use makes possible the description of discharge coefficient and jet angle. In Fig. from 7 to 14 the values determined for C_D and θ adopting Eq. 9, 12, 18 and 19 are plotted as a function of the square root of Reynolds number, as defined in Eq. 11.

The curves give a synthetic view of the characteristics analysed in the previous paragraphs, and allow a fairly good identification of the transition Reynolds number, as the limit value above which a flow can be considered as fully turbulent with a sufficiently high confidence level.

Figures 7 to 9 show that TYPE A notches, for all notch numbers, have a transition Reynolds number notably low (500÷900). The transition from the laminar to the transitional and turbulent efflux conditions is clearly defined, and the saturated values are stable. Beyond the transition value, discharge coefficients approach the values given by Eq. 9, and it is confirmed that intermediate openings (close to the area gradient discontinuity point) show values significantly lower than small and large openings. It is also worth noting that discharge coefficients for minimum and maximum

opening tend to get closer and closer as the number of notches increases. At the same time the jet angle at Reynolds number beyond the transition, approaches the value given by Eq. 19. This value is practically independent from the valve opening for each configuration and slightly increasing with the number of notches.

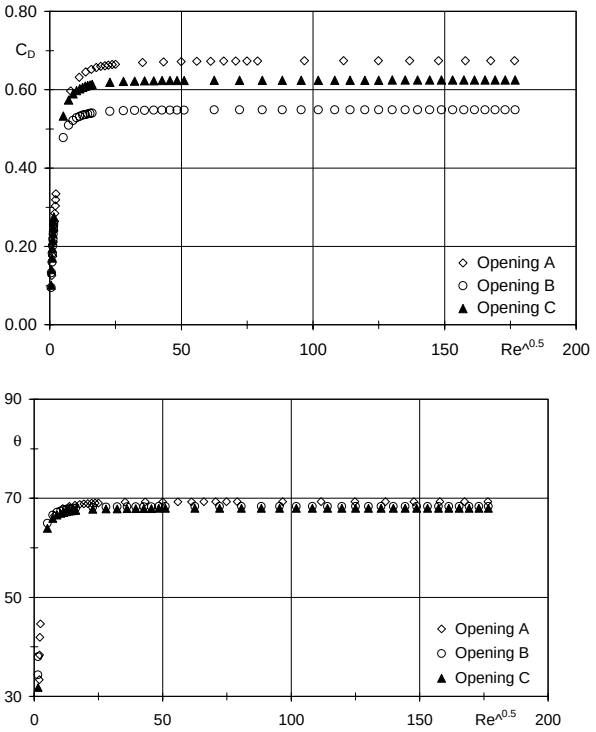

Fig. 7: *Discharge Coefficient and Jet Angle distributions with the Reynolds' Number variation – 2 notches TYPE A metering edge*

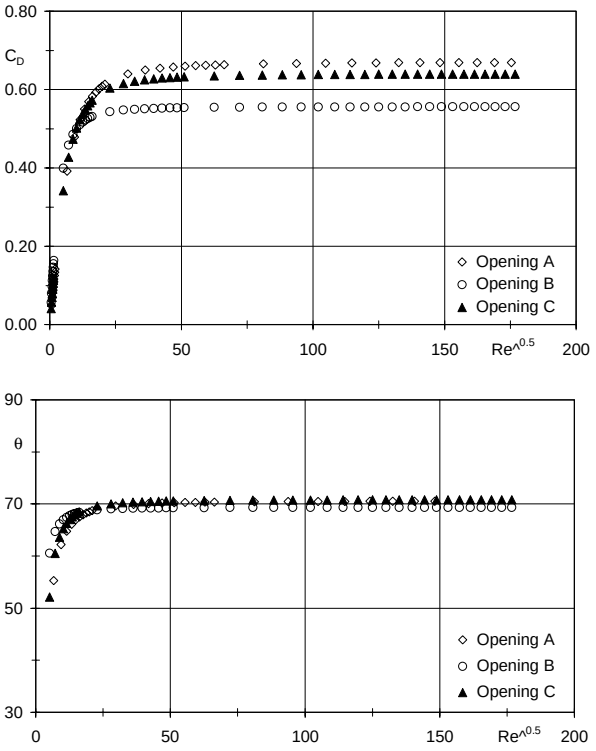

Fig. 8: *Discharge Coefficient and Jet Angle distributions with the Reynolds' Number variation – 3 notches TYPE A metering edge*

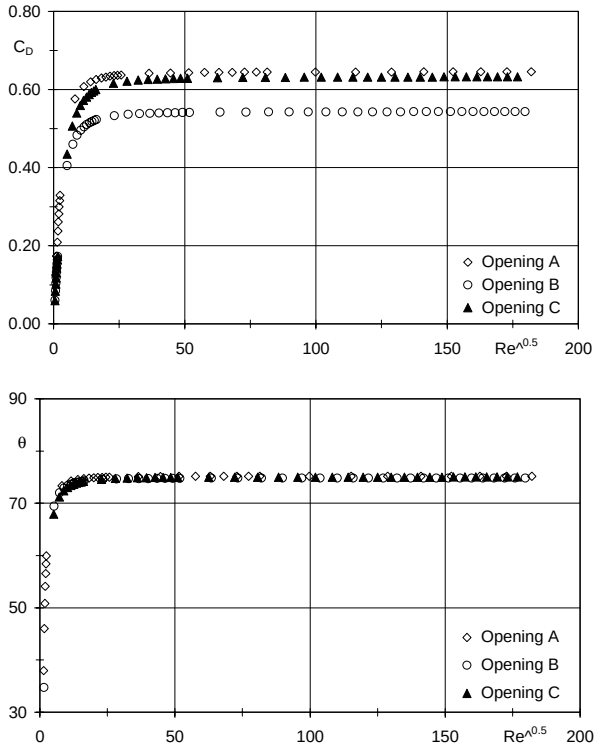

Fig. 9: *Discharge Coefficient and Jet Angle distributions with the Reynolds' Number variation – 4 notches TYPE A metering edge*

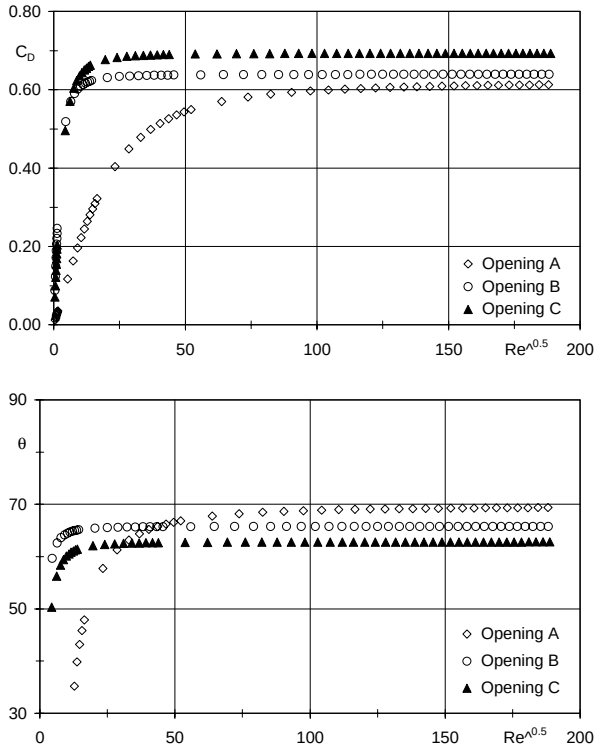

Fig. 10: *Discharge Coefficient and Jet Angle distributions with the Reynolds' Number variation – 2 notches TYPE B metering edge*

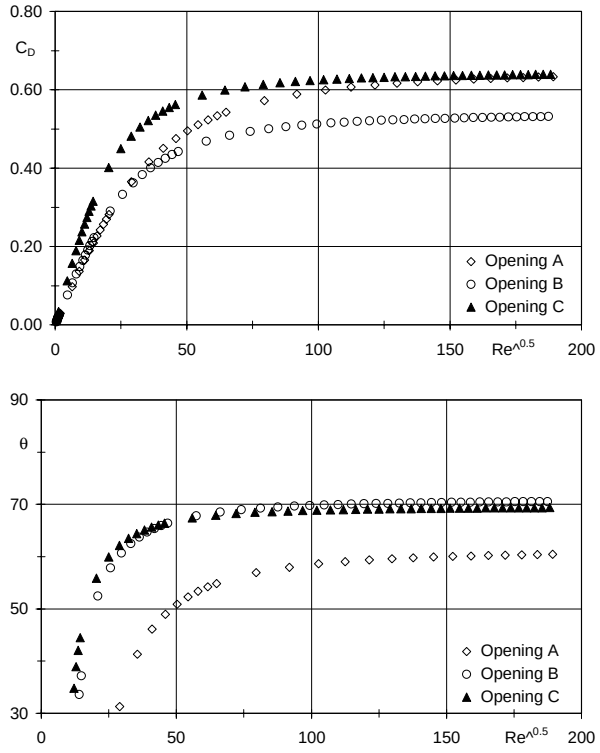

Fig. 11: *Discharge Coefficient and Jet Angle distributions with the Reynolds' Number variation – 3 notches TYPE B metering edge*

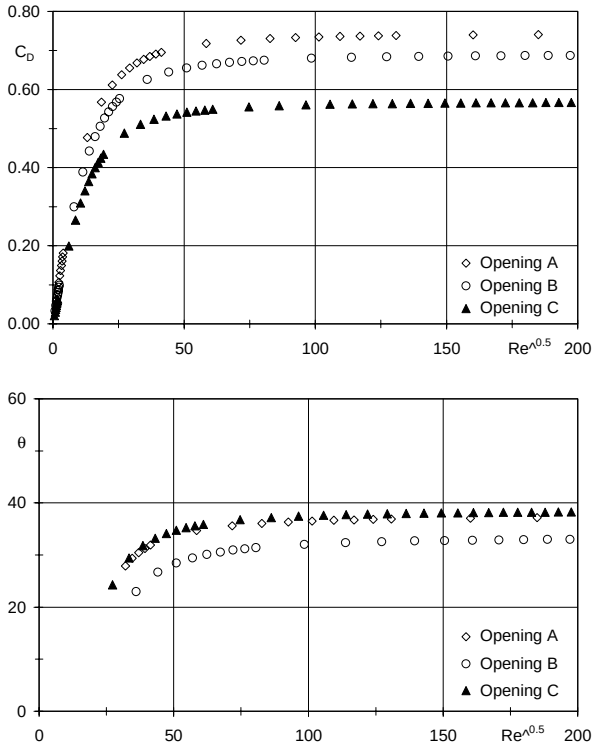

Fig. 13: *Discharge Coefficient and Jet Angle distributions with the Reynolds' Number variation – 2 notches TYPE C metering edge*

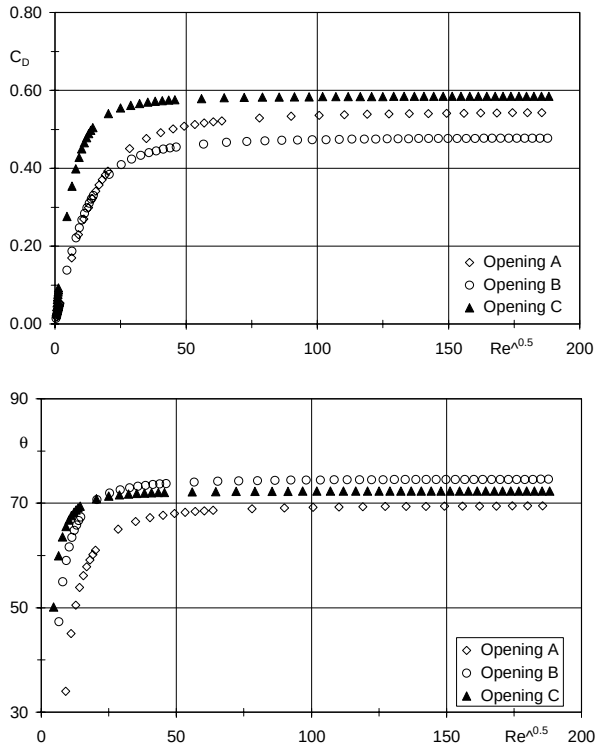

Fig. 12: *Discharge Coefficient and Jet Angle distributions with the Reynolds' Number variation – 4 notches TYPE B metering edge*

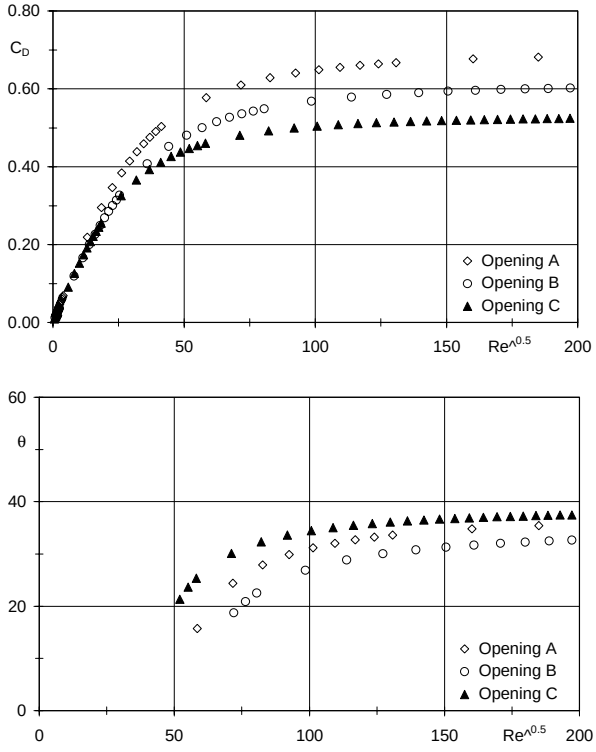

Fig. 14: *Discharge Coefficient and Jet Angle distributions with the Reynolds' Number variation – 4 notches TYPE C metering edge*

TYPE B notches give the characteristics plotted in Fig. 10 to 12. The observations introduced in the previous paragraphs on this type of notches apply also on these curves; however, the graphs seem to show a transition square root of Reynolds' number close to 75÷100, although in some cases it is not well identified. The differences among the various jet angles are more significant, when comparing the same configuration and for different configurations as well.

TYPE C notches plots are shown in Fig. 13 and 14. In this case the flow conditions can be considered saturated only for values of the square root Reynolds' number above 100. This limit is higher the higher is the number of notches. The jet angle tend to approach its asymptotic value only for Reynolds numbers particularly high, with the notable characteristic that, for all configurations, minimum and maximum opening have asymptotic values very close to each other and higher than those typical of intermediate openings.

5 Conclusions

This paper presents a thorough and critical analysis of stationary flow characteristics in different configurations of metering edges with timing notches, which are typically used in industrial hydraulic valves. The study is developed starting from experimental data gathered at different valve openings for eight different configuration of metering edges. The investigation allow to highlight trends and overall effects on discharge coefficient and jet angle of shape, number and position of timing notches. Among the main results shown in the paper, the effect of the discontinuities in area gradient are highlighted, together with the saturated flow conditions (asymptotic values of relevant flow parameters), where discharge and flow coefficients can be considered constant. It has been shown that the saturated values of the discharge coefficient are reached at values of the Reynolds number depending on shape and number of the notches on the metering edge, giving also some hints on how these indications can be used to improve valve design or to increase the effectiveness of valve metering characteristics.

Nomenclature

a, b, c, d, a_1, b_1	Polynomial coefficient
A	Area
F	Force
C_D	Discharge Coefficient
C_V	Velocity Coefficient
C_V^*	Flow Coefficient
D_H	Hydraulic diameter
S	Wetted Perimeter
R	Hydraulic Resistance
ρ	Fluid density
ν	Fluid kinematic viscosity
θ	Jet Angle

Subscript

AX	Axial component
EXP	Experimental
T	Turbulent
TH	Theoretical

Superscript

SAT	Saturation
Dp, Δp	Pressure drop
Q	Flow rate
Re	Reynolds number

References

Blackburn, J.F., **Reethof, G.**, **Shearer, J.L.** 1960. *Fluid Power Control*. M.I.T. Technology Press & John Wiley & Sons.

Borghi, M., **Cantore, G.**, **Milani, M.**, **Paoluzzi, R.** 1998. Analysis of Hydraulic Components Using Computational Fluid Dynamics Models. *Proceedings of the Institution of Mechanical Engineers, Part C, Journal of Mechanical Engineering Science*, Vol. 212 (7), Paper C09297, pp. 619-629.

Borghi, M., **Cantore, G.**, **Milani, M.**, **Paoluzzi, R.** 1997. Experimental and Numerical Analysis of Forces on a Hydraulic Distributor. *Proceedings of The Fifth Scandinavian International Conference on Fluid Power, SICFP '97*, Vol. I, pp. 83-98. Lingkoeping, Sweden.

Borghi, M., **Milani, M.**, **Paoluzzi, R.** 1999. Stationary and Dynamic Analysis of a Water Relief Valve. *The Fourth JHPS International Symposium on Fluid Power, JHPS '99*. Ariake, Tokyo, Japan.

Borghi, M., **Milani, M.**, **Paoluzzi, R.** 2000. Stationary Axial Flow Forces Analysis on Compensated Spool Valves. *International Journal of Fluid Power*. ISSN 1439-9776. Vol. 1, No. 1, pp. 17-25.

Elgamil, M. A. 2001. On the Dynamic Flow Forces of a New Class of Rotary Hydraulic Valves. *Proceedings of the Seventh Scandinavian International Conference on Fluid Power, SICFP'01*, ISBN 91-7373-056-4, Vol. 1, pp. 39-50. Linkoping, Sweden.

Ellman, A., **Piche, R.** 1996. A Modified Orifice Flow Formula for Numerical Simulation of Fluid Power Systems. *Proceedings of the Fluid Power Systems and Technology Division Sessions. ASME IMECE '96*, Vol. 3, pp. 59-63.

Gromala, P., **Domagal, M.**, **Lisowski, E.** 2002. Research on Pressure Drop in Hydraulic Components by means of CFD Method on Example of Control Valve. *Proceedings of the 2nd International FPNI Ph.D. Symposium on Fluid Power*. ISBN 88-88679-00-6. Modena, Italy.

Idelchick. 1983. *Handbook of Hydraulic Resistance*. Springer-Verlag.

Johnston, D.N., **Edge, K.A.**, **Vaughan, N.D.** 1991. Experimental Investigation of Flow and Force

Characteristics of Hydraulic Poppet and Disk Valves. *Proceedings of the Institution of Mechanical Engineers, Part A, Journal of Power and Energy*, Vol. 205, pp. 161-171.

Lugowsky, J. 1993. Experimental Investigation on the Origin of Flow Forces in Hydraulic Piston Valves. *10th International Conference on Fluid Power*, BHR. Brugges, Belgium.

Merrit, H. E. 1967. *Hydraulic Control Systems*. John Wiley & Sons.

Palumbo, R., **Paoluzzi, M.**, **Borghi, M. Milani.** 1996. Forces on a Hydraulic Valve Spool. *Proceedings of the Third JHPS International Symposium on Fluid Power*, pp. 543-548. Yokohama, Japan.

Del Vescovo, G., **Lippolis, A.** 2002. Flow Forces Analysis on a Four-Way Valve. *Proceedings of the 2nd International FPNI Ph.D. Symposium on Fluid Power*. ISBN 88-88679-00-6. Modena, Italy.

Viersma, T.J. 1980. *Analysis, Synthesis and Design of Hydraulic Servosystems and Pipelines*. Elsevier Scientific Publishing Co.

Wu, D., **Burton, R.**, **Schoenau, G.** 2002. An Empirical Discharge Coefficient Model for Orifice Flow. *International Journal of Fluid Power*. ISSN 1439-9776. Vol. 3, No. 3, pp. 13-18.

Wu, D., **Burton, R.**, **Schoenau, G.**, **Bitner, D.** 2003. Modelling of Orifice Flow Rate at Very Small Openings. *International Journal of Fluid Power*. ISSN 1439-9776. Vol. 4, No. 1, pp. 31-39.

MASSIMO BORGHI
Born in Modena, 1956. Graduated cum Laude in Mechanical Engineering in 1981 at the University of Bologna. Researcher at the Faculty of Engineering in Bologna from 1983 to 1998. Associate Professor at the Faculty of Engineering in Modena from 1998 to 2001. Full Professor at the Faculty of Engineering in Modena since November 2001.
Author of more than 60 scientific papers, concerning energy conversion systems, fluid power applications and components and internal combustion engines. Actually, his research activity is particularly involved in the prediction of the steady and transient characteristics of positive displacement pumps and motors (external gears units, vane units and axial piston ones), in the fluid dynamic optimization of on-off and proportional control valves metering characteristics, and in the optimization of the dynamic response of electro-hydraulic circuits for mobile applications.

MASSIMO MILANI
Born in Modena in 1968. Graduated in Materials Engineering at the University of Modena in 1994. PhD in Materials Engineering at the University of Modena in 1998. Researcher at the Faculty of Engineering of the University of Modena from November 1999 to November 2002. Researcher at the Faculty of Engineering in Reggio Emilia from December 2002. Member of FPNI and SAE.
Author and Co-Author of more than 40 papers dealing with the design of positive displacement pumps and motors, with the steady and transient characterization of on-off and proportional hydraulic components, with the development of gasoline and diesel injection systems and with the dynamic analysis and design of hydraulic equipment for automotive and off-road applications.

ROBERTO PAOLUZZI
Born in Ferrara in 1961. Graduated in Nuclear Engineering at the University of Bologna in 1986. Senior Researcher at IMAMOTER - C.N.R. Institute with interests in fluid power systems, control and simulation and in computational fluid dynamics.
Deputy General Secretary for Europe-Africa of ISTVS (International Society for Terrain-Vehicle Systems). Member of ASME and FPNI. Chairman of ISO/TC 127/SC 4 since 1991.
Author of more than 160 papers and technical reports in fluid power systems technology and Earth Moving Machinery parts and components design.